CHAPTER 3:

METHODOLOGY

CHAPTER 3

METHODOLOGY

3.1 Introduction

This chapter consists of three subtopics, $Li_4Ti_5O_{12}$ and composite preparation, characterization, electrochemical cell construction and performance. The precursor of $Li_4Ti_5O_{12}$ was synthesized via the sol-gel method and followed by film formation using poly (vinyl alcohol) PVA polymer by casting technique. The prepared $Li_4Ti_5O_{12}$ and polymer composite with $Li_4Ti_5O_{12}$ were characterized using electrochemical impedance spectroscopy (EIS), fourier transform infra-red (FTIR) spectroscopy, x-ray diffraction (XRD), UV-Visible spectroscopy and scanning electron microscopy (SEM). $Li_4Ti_5O_{12}$ was applied in an electrochemical cell and the performance of cell studies.

3.2 Sample Preparation

3.2.1 Powder synthesis

Lithium tert-butoxide (purity 97%) was procured from Fluka and titanium isopropoxide (purity 97%) from Aldrich. 0.05 mole of lithium tert-butoxide was dissolved in ethanol. This was followed by the addition of 0.03 mol of titanium isopropoxide. A light yellow solution appeared after addition of titanium alkoxide. After mixing with a mixture ethanol and water, the light yellow solution turned to white. After keeping the white solution for one week at room temperature, the solution was filtered and the residue was collected by filtering the sample. The sample was calcined at 100 ^oC and then at 700 ^oC, 800 ^oC, 900 ^oC and 1000 ^oC for one hour followed by sintering at 800 ^oC for two, three,

four and five hours. Figure 3.1 summarizes the experimental activities for sample preparation.

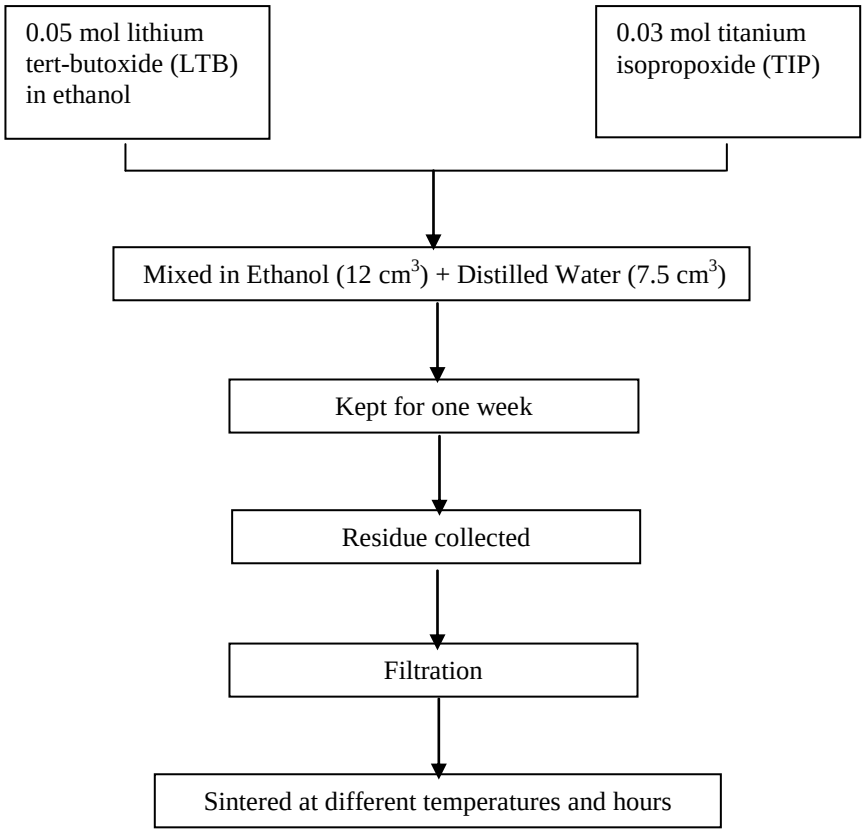

Figure 3.1: Powder synthesis flowchart.

3.2.2 Composite film

0.5 g poly (vinyl alcohol) (PVA) was dissolved in 50 mL 1 % acetic acid. Then, lithium titanium oxide was added into the solution according to the concentrations in weight percentage (wt. %) as listed in Table 3.1. The mixture was stirred for 24 hours. The mixture was cast into plastic petri dish and left to evaporate. The dried film was kept in the dry state in desiccators.

Table 3.1: Composition of composite film studied in this work.

Weight of PVA (g)	Weight percentage (wt. %) of $Li_4Ti_5O_{12}$	Weight of lithium titanate (g)
0.5	2	0.0102
0.5	4	0.0208
0.5	6	0.0319
0.5	8	0.0435
0.5	10	0.0556

3.3 Sample characterizations

3.3.1 Thermo gravimetry mass analysis

Thermal studies are very important in order to determine whether the prepared sample can be thermally stressed or inert towards heat. Thermo gravimetry analysis (TGA), differential scanning calorimetry (DSC) and differential thermal analysis (DTA) are promising tools to study the thermal behavior of samples such as in the present work. Results from these tools can be combined with results from mass spectroscopy (MS) and fourier transform infrared (FTIR) to obtain valuable information for more detailed interpretation of the thermal properties of the sample [Madarász *et al*., 2007; Nouwen *et al*., 1996]. As an example, TGA coupled with an evolved gas analyzer (EGA) enable the determination and identification of released gases and allows the calculation of weight losses [Mullens *et al*., 2002]. The mechanism of product formation can be inferred.

TGA-MS was employed in this work to determine the temperature at which the mass of the heated precursor will be constant. The dissociation reaction of the precursor

corresponds to the loss in weight at certain temperatures [Ibrahim and Abu-Ayana, 2008]. Figure 3.2 and 3.3 show TG-DSC-MS thermogram of N-Al-codoped precursor. Zhang (2009) identified in the range of 100 ^{o}C-200 ^{o}C, a large mass-loss step and a distinct exothermic peak at 165.1 ^{o}C corresponding to the H_2O (m/z= 18) and NH_3 (m/z=17) evaporation as detected in the mass spectra shown in Figure 3.3.

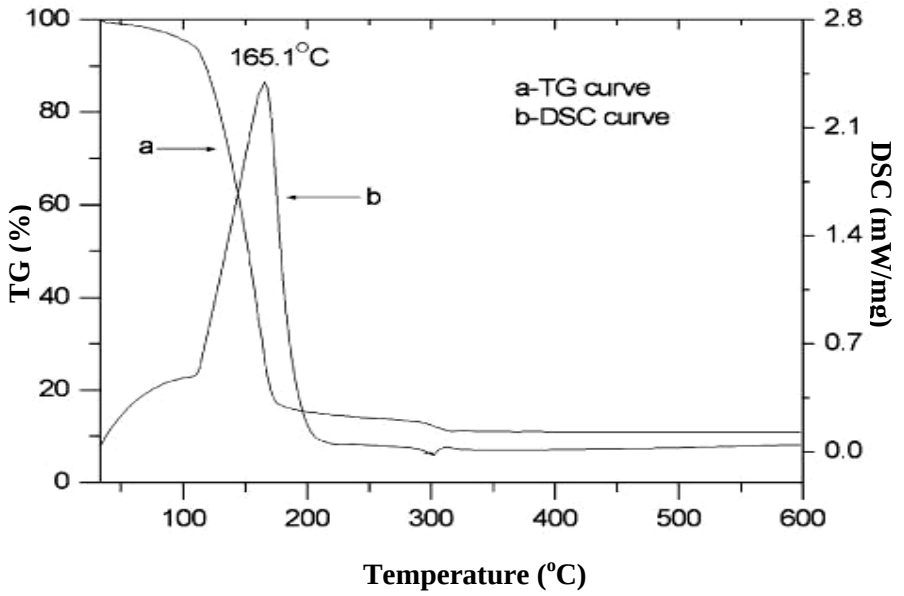

Figure 3.2: TG and DSC curves of the codoped precursor solution with Zn:N:Al=1:3:0.05 [Zhang, 2009].

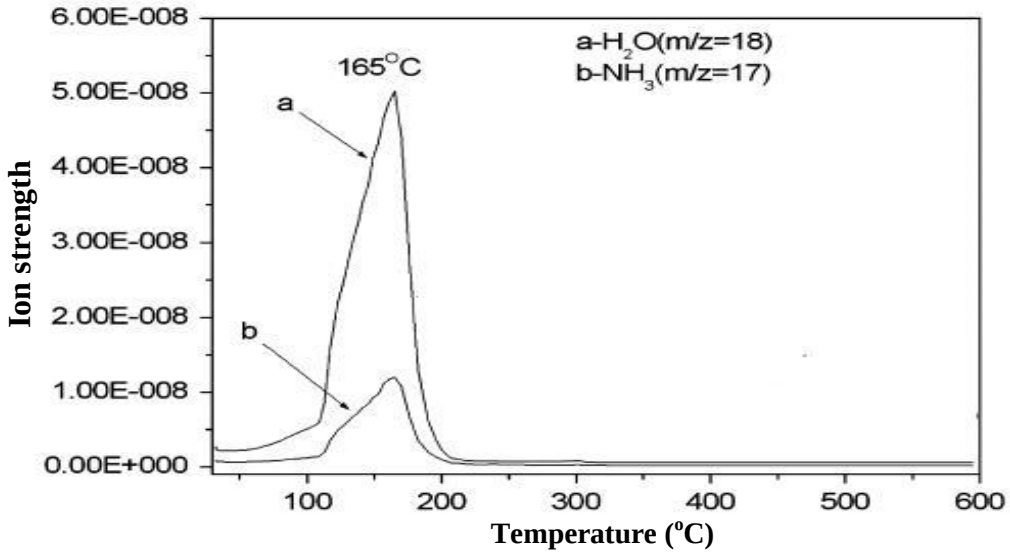

Figure 3.3: Mass spectra of HN_3 and H_2O in the resultant gases of the codoped precursor solution [Zhang, 2009].

For this work, the precursor was put in a pan and heated from 30 ^{o}C to 1000 ^{o}C under nitrogen flow at 50 mL min^{-1}. The heating rate was 10 ^{o}C min^{-1}.

3.3.2 X-ray diffraction (XRD)

XRD was employed to study the nature of prepared samples whether it is amorphous, crystalline or both [Majid and Arof, 2005]. When x-rays are directed on a specimen, the x-rays are scattered by electrons present in the material. If the scattering results in maxima and minima in the diffracted intensities the material is crystalline. During an x-ray diffraction (XRD) measurement the angles of incidence and detection are scanned. When the intensity of detected x-rays is plotted as a function of angle θ an x-ray diffraction pattern characteristic for the sample material is obtained. The usual depth of XRD measurements ranges from a few micrometers to a few hundred micrometers, depending on the density of the material. By using a very small, fixed incidence angle of the x-rays (so-called grazing incidence measurement) thin layers of only a few nanometers can be investigated.

The broad peak appearing on the diffractogram implies a non-crystalline or amorphous compound. The sharp and narrow peaks correspond to crystal structure. Figure 3.4 shows the XRD patterns of $LiNi_{0.3}Co_{0.7}O_2$ that has been sintered at different temperatures. It can be observed that, all diffractograms exhibit narrow and sharp peaks indicating that the sintered samples are crystalline. Bragg's equation was used to calculate spacing distance (*hkl*) between the atomic layers of the cubic structure [Shokrollahi, 2009].

$$n\lambda = 2d_{hkl}\sin\theta \tag{3.1}$$

Here n is 1, λ is the wavelength of the incident x-ray beam which is 1.5406 Å and θ is the incident angle.

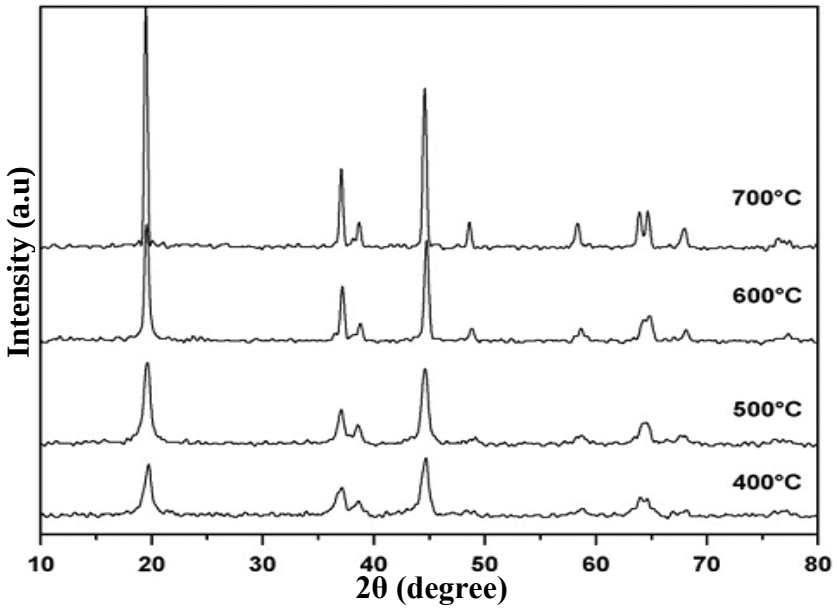

Figure 3.4: XRD patterns of $LiNi_{0.3}Co_{0.7}O_2$ sintered at different temperatures [Hernandez *et al*., 2008].

The lattice parameter can be calculated using the equation

$$d_{hkl} = \frac{a}{\sqrt{h^2 + k^2 + l^2}} \tag{3.2}$$

where a is the lattice parameter and (hkl) are the Miller indices describing a particular set of planes.

In this work, the structure of the products was examined by X-ray diffractometry (XRD) and measurements were carried out using Siemens D5000 with Cu Kα radiation (λ = 1.5406 Å) in the 2θ angle range from 5^o to 80^o.

3.3.3 Electrochemistry impedance spectroscopy (EIS)

Impedance spectroscopy is a powerful tool to determine the bulk resistance and hence the ionic conductivity. Impedance is a complex quantity made up from real (Z_r) and imaginary (Z_i) parts as shown in Equation (3.3).

$$Z = Z_r + Z_i \tag{3.3}$$

The real and imaginary parts can be written as Equation (3.4) and (3.5) respectively

$$Z_r = Z_o \cos\phi \tag{3.4}$$

$$Z_i = Z_o \sin\phi \tag{3.5}$$

Both real (Z_r) and imaginary (Z_i) parts can be presented in the form of a Cole-Cole plot where $-Z_i$ is plotted versus Z_r as shown in Figure 3.5.

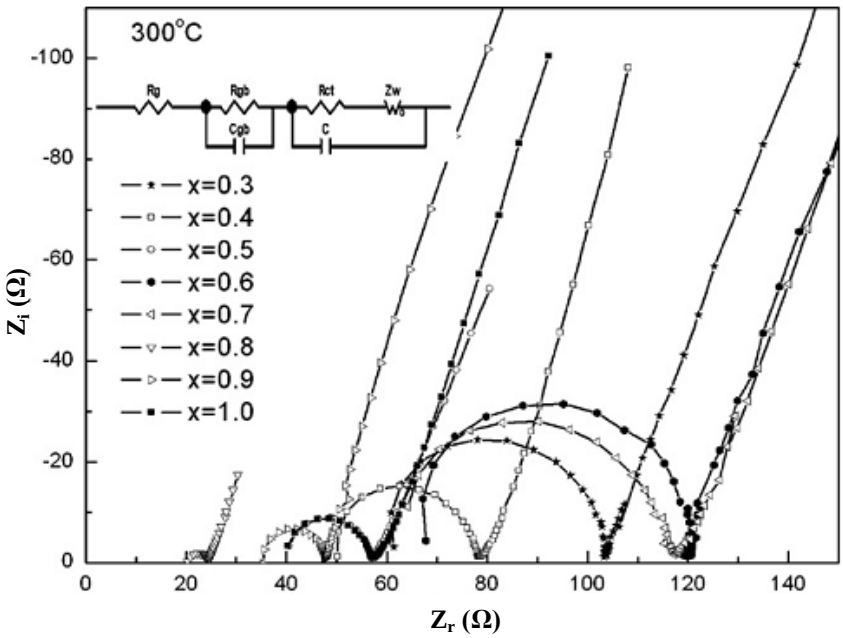

Figure 3.5: Complex impedance plot at 300 ^{o}C for the $Na_{1+x}Al_xGe_{2-x}P_3O_{12}$ glass–ceramics calcined at 800 ^{o}C for 18 hours and the equivalent circuit is shown on the top left corner [Zhang *et al.*, 2009].

As can be seen in Figure 3.5 the horizontal and vertical axes are drawn with the same scales. This is to ensure the correct type of equivalent circuit is inferred. The equations for the dielectric constant (ε_r), the dielectric loss (ε_i), the real electrical modulus (M_r),

the imaginary electrical modulus (M_i) and dissipative loss (tan δ) can be shown as below [Majid and Arof, 2007].

$$\varepsilon_r = \frac{Z_i}{\omega C_O (Z_r^2 + Z_i^2)} \tag{3.6}$$

$$\varepsilon_i = \frac{Z_r}{\omega C_o (Z_r^2 + Z_i^2)} \tag{3.7}$$

Here $C_o=\varepsilon_o A/t$. ε_o is permittivity of the free space, A is the electrolyte-electrode contact area, t is thickness of the sample and $\omega=2\pi f$, f being the frequency in Hz.

$$M_r = \frac{\varepsilon_r}{(\varepsilon_r^2 + \varepsilon_i^2)} \tag{3.8}$$

$$M_i = \frac{\varepsilon_i}{(\varepsilon_r^2 + \varepsilon_i^2)} \tag{3.9}$$

Dissipative loss can be expressed as following equation

$$\tan\delta = \frac{\varepsilon_i}{\varepsilon_r} \text{ or } \frac{M_i}{M_r} \tag{3.10}$$

In this work, the HIOKI 3531-01-LCR Hi-Tester was employed and operated in the frequency range from 50 kHz to 100 kHz. Temperature studies were carried out from 25 ^{o}C to 120 ^{o}C. Samples were sandwiched between two stainless steel electrodes under spring pressure.

3.3.4 Fourier transform infrared (FTIR) spectroscopy

Infrared spectroscopy is a qualitative and quantitative device based on the vibrations of the atoms of a molecule whether stretching or bending. Osman and Arof (2003) pointed that FTIR spectrum gives valuable information such as band properties, frequencies, intensity and hence chemical processes involved can be analyzed. An infrared spectrum can be obtained by passing infrared radiation through a sample and determining what fraction of the incident radiation is absorbed at a particular energy. The energy at which

any peak in an absorption spectrum appears is represented by the wave number of a vibration of a part of a sample molecule. Fourier transform infrared (FTIR) spectroscopy was employed to investigate the occurrence of complexations occurred in the system. The wavenumber is in the range of 400 cm^{-1} to 4000 cm^{-1}. The resolution of this work is 1 cm^{-1}.

3.3.5 Scanning electron microscope (SEM)

The scanning electron microscope was used to study the morphology of materials. The operation of SEM is initiated by the bombardment of electrons on the target sample. In this work, particle of $Li_4Ti_5O_{12}$ and composite films were adhered to the top of sample holder with double-sided conductive tape.

3.3.6 UV-Vis spectroscopy

The ultraviolet-visible (UV-Vis) spectrophotometer is an instrument used in the laboratory that analyzes compounds in the ultraviolet (UV) and visible (Vis) regions of the electromagnetic spectrum. This instrument focuses on the electronic transitions. The wavelength and maximum absorbance of compounds can also be determined through this instrument. Figure 3.6 shows the UV-Visible absorption spectra of pure PVA as well as PVA doped with different concentrations of $TiCl_3$.

It is clear that the spectrum of pure PVA exhibits an absorption edge (AE) around 250 nm indicating the semi-crystalline nature of PVA and also shows a shift in AE towards the higher wavelengths. In this study, PVA and composite films were scanned using the via Perkin Elmer UV-Visible spectrophotometer in the range of 200 nm to 900 nm at room temperature.

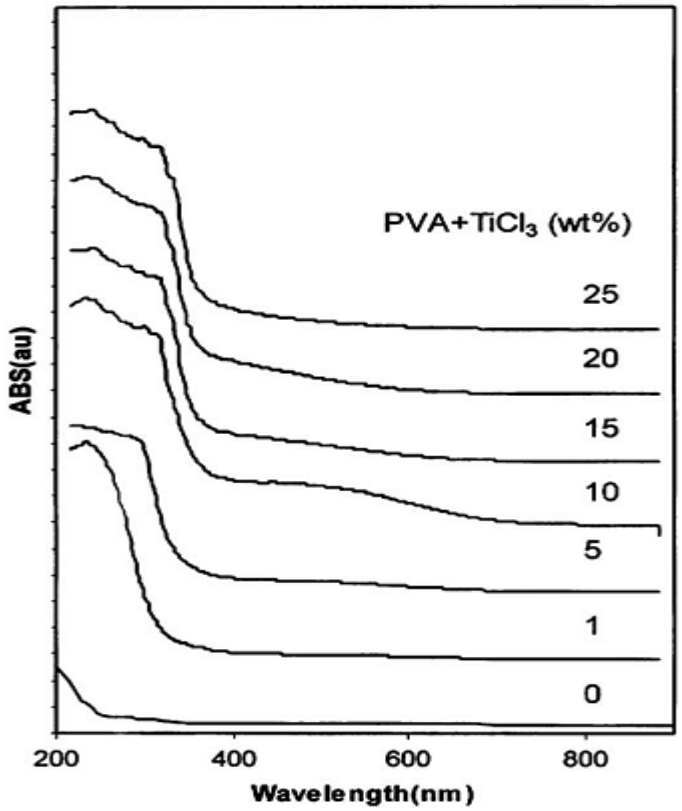

Figure 3.6: The variation of the absorption with the wavelength for different concentrations of $TiCl_3$ [Abdelaziz and Ghannam, 2010].

3.4 Electrochemical cell fabrication and characterization

The cell consists of a lithium metal electrode, a $Li_4Ti_5O_{12}$ electrode material and a commercial electrolyte, 1M $LiPF_6$ in a 1:2 (v/v) mixture of ethylene carbonate (EC) and diethyl carbonate (DEC), Figure 3.7. Lithium metal behaved as quasi reference and auxiliary electrodes [Ganesan *et al*., 2007].

The $Li_4Ti_5O_{12}$ electrode contains:

(i) 85 wt % of $Li_4Ti_5O_{12}$

(ii) 15 wt % of Teflon acetylene black (TAB)

All these materials were homogenously ground together using mortar and pestle until the mixture form a thin compact. The sampel was pasted on the copper foil and heated in the oven at 100 ^oC for two hours to eliminate moisture. The battery was constructed

in a LABmaster 130 Mbraun Ar-filled glove box. The cell was characterized using LG-Bas potentiostat-galvanostat equipment and discharge current is 0.5 mA.

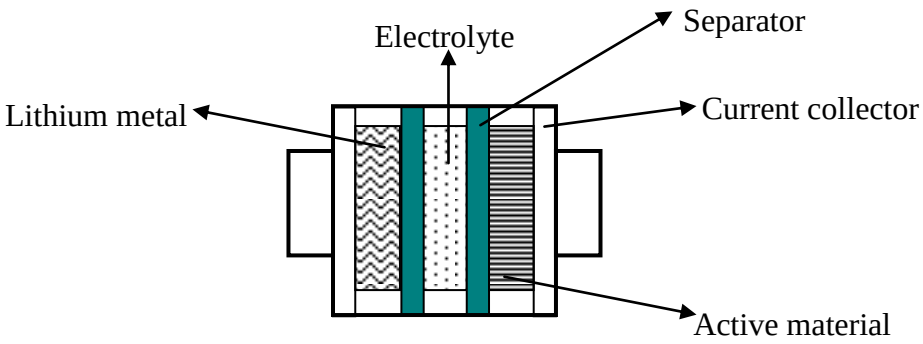

Figure 3.7: The systematic diagram of cell construction.

3.5 Summary

In this work, $Li_4Ti_5O_{12}$ will be prepared by the sol-gel technique. The prepared sample will be analyzed using thermo gravimetric analysis (TGA) and x-ray diffraction (XRD). $Li_4Ti_5O_{12}$ was applied as anode material in a lithium half cell and charge-discharge characteristics will be studied. PVA films doped with different concentrations of $Li_4Ti_5O_{12}$ will be prepared by solvent casting technique. The film will be characterized using x-ray diffraction (XRD), fourier transform infrared (FTIR), UV-Vis spectroscopy, scanning electron microscopy (SEM) and electrochemical impedance spectroscopy in order to study the effect of $Li_4Ti_5O_{12}$ addition to the polymer.